A fast defect detection algorithm for glass tube based on ROI reduction

Gabriele Antonio De Vitis, Pierfrancesco Foglia and Cosimo Antonio Prete
Dipartimento di Ingegneria dell'Informazione, Università di Pisa
Pisa, Italy

ABSTRACT

In this paper, we present an algorithm for defect detection in glass products that allows us to minimize the processing time. The main idea is based on the reduction of the size of the image area to investigate by using the features of glass images. The proposed solution doesn't compromise the quality of detection and allows us to achieve a performance gain of 66% in terms of processing time, and 3 times in term of throughput (frames per second), in comparison with standard algorithms for defect detection.

Keywords: Defect detection, glass production, real-time inspection, image processing, inspection systems.

1. INTRODUCTION

An inspection system for semi-finished glass production can be based on machine vision [1], [2], [3] and it is constituted by an Image Acquisition Subsystem and a Host Computer. The Image Acquisition Subsystem is devoted to the acquisition of the digitized images (frames); key components of such system are a LED-based illuminator, a line scan camera, and a frame grabber, which groups together single sequential lines captured by the camera into a single frame, transferring it to the Host Computer. The Host Computer implements defect detection and classification algorithms and it takes the discard decisions, communicating them to a Cutting and Discarding Machine [4]. Discard decisions are taken considering process parameters, some of which are settled via a usable operator GUI [5].

The evolution of the glass production process requires both high accuracy in defects detection and faster production lines. The detection and classification of defects imposes temporal constraints on the system. The inspection system, in fact, works in pipeline, and the Image Acquisition Subsystem feeds the pipeline at a rate which is determined by the sampling rate of the line scan camera divided by the number of lines in a frame. The Defect Detection and Classification module must work with the same rate, to avoid frame loss, i.e., the sampling rate of the line scan camera enforces an upper bound to the processing time of defect detection and classification algorithms. The current requirement of increasing the production speed involves the use of line scan cameras with increased sampling rate to keep constant or to improve the accuracy of defects detection. Consequently, the increase of production speed determines the need to reduce the processing time of defect detection and classification algorithms.

To reduce the processing time of defect detection and classification algorithms, in this paper we propose an algorithm that reduces the size of the images to be investigated by excluding subareas that can be assumed to not include defects.

As an example, we consider the critical production of glass tubes, converted into pharmaceutical containers such as vials, syringes, and carpules.

Due to imperfections in the raw materials used in the furnace, this type of glass may have defects such as knot inclusions (blobs) or flexible fragments called lamellae, which can cause subsequent problems and pharmaceutical recalls [6], [7], [8]

The main classes of defects relevant for pharmaceutical glass production [1], [9] due to critical size features and their significant effects on the final quality of the tubes are:

1) air lines due to the presence of air bubbles in the furnace which are pulled by the drawing machine; they appear as darker lines of long dimensions with a back illuminator, with the end parts thinner than the center one. This line, when it is too close to the tube surface, breaks and therefore is thinner and more difficult to detect.
2) knot inclusion (blobs) due to imperfections in the raw materials used in the furnace; they appear on the tube surface as circular lenses, while they appear on the captured image as dark patches, orthogonal to the frame.

Results of experimental evaluation on such inspection system show that the proposed solution achieves an 66% reduction in processing time during the detection/classification phase and improvements of 3x in term of frames per seconds, with the same accuracy in defect detection. We characterize also the effects of the parameters of the algorithm on processing time and quality of detection and propose a procedure to determine upper bound to these parameters.

The paper is organized as follow: in Section 2, we present the state of the art related to the system, and in Section 3 we present the rational of the proposal. In Section 4, we explain the proposed algorithm and we report the experimental results in Section 5. Conclusion are given in Section 6.

2. STATE OF THE ART

As usually done in inspection systems, the set of elaborations performed on each frame can mainly be divided into 3 stages [2], [10], [11].

1. Image preprocessing
2. Defects detection
3. Defects classification

In the pre-processing phase, algorithms are used to prepare the image for the following stages, with the aim of reducing detection errors due to the acquisition process and/or speeding up the calculation by excluding the regions not to be investigated. The steps generally adopted concern noise reduction, contrast enhancement [12], elimination of unwanted regions and identification of the region of interest (ROI).

In glass tube production, state-of-the-art ROI extraction techniques consist in identifying the visible part of the tube inside the frame (called hereinafter Internal of the tube), excluding also the dark area due to the glass surface on which the light rays of the illuminator have a critical angle of incidence according to Snell's law, are reflected on the glass tube and do not affect the camera sensor. An algorithm to extract the internal part of the tube has been proposed in [1].

In the defect detection stage, algorithms are used to determine image regions whose pixels may identify a defect To extract these regions, segmentation techniques are adopted [10], typically based on thresholds [3] or on edge detection [13], [14].

The classification stage consists of algorithms that extract a series of characteristics of the segmented regions, eventually including them within predetermined classes of defects.

State of the art techniques for feature/defect detection and extraction are the edge detection techniques [13]. Edge detection aims to identify points in a digital image where the image brightness changes sharply compared to the rest. Among the various edge detection techniques, the algorithm proposed by Canny [14] (Canny algorithm) is considered the ideal one for images with noise [13]. The image is first smoothed with a Gaussian filter and then gradient magnitude is computed at each pixel of the smoothed image; edges are determined by applying non-maximum suppression, double threshold, and hysteresis. The algorithm has been usefully adopted in various applications domains (inspection of semiconductor wafer surface [15], detection of defects in satin glass [16], measuring icing shape on conductor [17], studies on bubble formation in co-fed gas-liquid flows [18]) and it has been also adopted for the detection of defects in similar inspection systems [1]

Other techniques for defect detection and extraction are based on thresholds, that can be global (fixed for the whole image) or local, i.e. they can be variable in different regions of the image [19].

As for global thresholds techniques, [12] presents an inspection method for float glass fabrication. The authors utilize a benchmark image to remove bright and dull stripes that are present in their glasses. Then, they utilize adaptive global thresholds based on the OTSU algorithm [20] to separate distortions from defects. The OTSU algorithm selects threshold values (one for each image) that maximize the inter-class variance of the image histogram [21]. It is useful for separating background from defects/foreground and produces satisfactory results when images present bimodal or multimodal histograms [10]. It has been successfully utilized in [10] to derive a configurable industrial vision system for surface inspection of transparent parts (in particular, it has been tested on headlamp lens) and again in [22] to detach defects from the background in a float glass defect classificatory and in [23] or glass inspection vision systems.

By considering the characteristics of the tube glass production, the use of single or multiple constant thresholds does not allow the detection of defects (Fig.3b highlights that the luminous intensity of columns belonging to the defect is similar to the ones of columns not including a defect). Besides, techniques based on background subtraction or other template matching techniques [3],[24] cannot be utilized due to the tube vibration and the not perfect circular section of the tube (the "sausage" shape).

As for local thresholds techniques, the Niblack's [19] binarization method is a local adaptive thresholding technique, based on varying threshold over the image by using local mean value and the standard deviation of gray level evaluated in a window centered in each pixel. This method can separate the object or text from the background effectively in the areas near to the object. Niblack method is one of the document segmentation methods and has shown good results in segmenting text from the background. Anyway, it can be applied also to images without text [25] and has been applied in a vision system for auto seeding and for observing the surface of the melt in the Ky method for the Sapphire Crystal Growth Process [26]. In the Niblack's approach, noise still occurs in a varying manner in the background; different improvements over the original paper have been proposed, which work to improve detection or reduce the processing time [19]. Examples are the approach presented in [27], that proposes new thresholds to limit noise, and in [28] that applies a global threshold to each sub-image and not to each single pixel to reduce processing time.

All these techniques extract a ROI from the acquired image. This extraction removes the part of the image that is not part of the inspection object (for example the portion of image that does not contain the tube, as in [1], or the image of the roller conveyor that is separated from the glass in [16]) but do not use information on defects to further reduce the ROI. Only in [23] is presented a technique that identifies not defective areas within the ROI (background) using a threshold on the local variance calculated in a window centered on a pixel (values of the variance lower than a threshold identify regions without defect).
In this paper, statistics on areas without error are used to automatically calculate the thresholds to perform segmentation, more accurately than OTSU. In our work, we use the knowledge of the no defective areas to reduce the size of the ROI and, therefore, the execution time. We exploit a double threshold mechanism with hysteresis to further limit the size of the ROI, and we perform columns elaboration as they have an almost constant distribution of luminous intensity, thus avoiding the introduction of further expensive filtering.

3. THE ROI EXTRACTION

In the ROI Extraction stage, two areas are excluded from the image as they do not contain useful information: i) areas outside the tube and ii) dark areas near the edges of the tubes. Near the edge of the tube, in fact, light rays generated by the illuminator reflect on the glass tube, having a critical angle of incidence according to the Snell's law, and do not affect the camera sensors (Fig. 1).

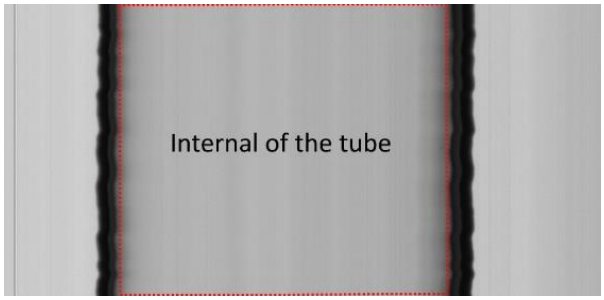

Fig. 1. Image taken by the line-scan camera. The array of CCD sensors in the line scan camera is orthogonal to the direction of the movement of the tube (tube direction). The internal of the tube is also highlighted. It represents the portion of the image which is further analyzed for detecting the column with defect for segmentation. The frame is composed of 1000x2048 pixels.

Our main requirement is to reduce the overall processing time. To achieve this goal, our idea is to remove areas where it is possible to easily predict that no defects are present (reducing the size of the ROI). State of the art defect detection techniques examine the entire internal area of the tube. They waste processing time if it is known that some of these parts do not contain defects.

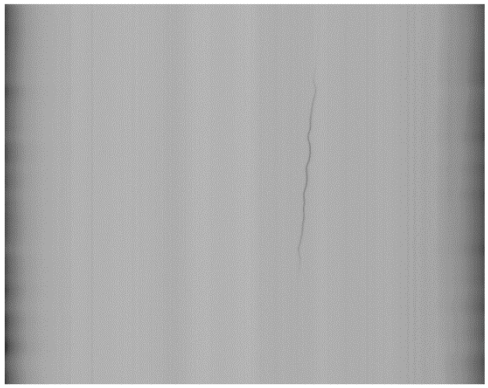

(a)

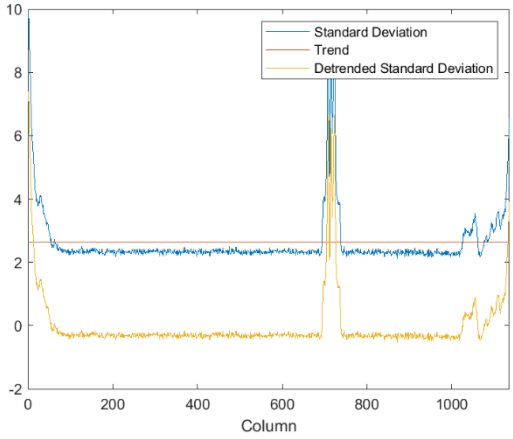

(b)

Fig. 2a-b: a) Internal part of the tube including an air line. b) Standard Deviation, Linear Trend and DSD of columns of figure a).

To reduce the size of the ROI, we observe that, since the luminous intensity inside a column is almost constant except in pixels where there is noise or defects, the standard deviation of each column can be used as an indicator of the presence of a defect on that column, as shown in Fig. 2b. Therefore, values of the standard deviation of a column below a certain threshold indicate that the column can be excluded by the following elaborations. Anyway, the standard deviation of the columns is also influenced by the alignment of the illuminator with the acquisition camera. In case of not perfect alignment, the standard deviation shows an increasing trend from one edge of the tube to the other, which can be approximated with a linear trend (Fig. 3b). In order not to have any influence from this factor, we consider the values of the standard deviation of the columns removing their linear trend (Detrended Standard Deviation - DSD).

Another relevant requirement concerns the ability to accurately detect the size of defects. We have experimented that luminous intensity of the defects presents high values near the central area of the defects but tends to decrease away from it. Therefore, not all the columns including a defect have high standard deviation value. Applying a single threshold on the DSD can then lead to an inaccurate detection of the size of the defects. Anyway, a defect includes columns with DSD over a certain threshold, and columns adjacent to those with lower DSD values. To detect these columns, we apply two hysteresis thresholds (t_L and t_H with $t_L<t_H$) algorithm. Columns with DSD values less than t_L are not considered to belong to ROI, columns with values greater than t_H are considered to belong to ROI and column with values between t_L and t_H are considered to belong to ROI only if they are adjacent to columns that belong to ROI (Fig. 4).

Using DSD criterion, areas near the edge of the tube are often classified as ROI, as they have peaks of DSD greater than the peaks of the DSD of the columns where defects are placed. These values are caused by many effects as the vibration of the moving tube or the imperfect circular shape of the tube. In these areas, there may be defects that if included in the ROI will be recognized by the "Defect Detection and Classification Subsystem". The solution is to exclude the ROIs located near the edges. This solution is not destructive because, in the case of glass tube, 3 cameras and illuminators are utilized to have a 360 degrees inspection, and areas near the edges for a camera appear in central area for one of the other two (positioned at 120 degrees from it and the tube). So, the solution to exclude areas near the edge of the tube seems the most appropriate to reduce performance needs of the algorithms.

(a)

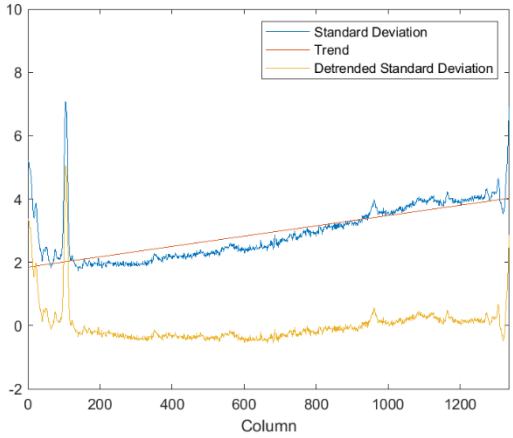

(b)

Fig. 3a-b: a) Internal part of the tube including a blob. b) Standard Deviation, Linear Trend and DSD of columns of figure a).

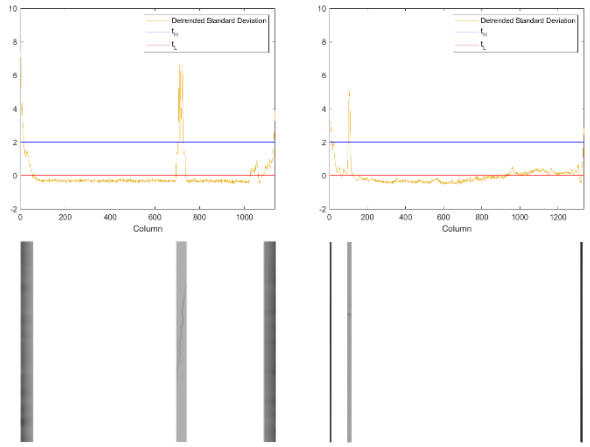

Fig. 4: Application of two thresholds with hysteresis to the DSD of column of Fig 2a and 3a. Above is shown the ROIs of images in Figure 2a and 3a as results by applying the proposed algorithm.

4. ALGORITHM

The proposed algorithm (Detrended Standard Deviation ROI Reduction algorithm, DSDRR), starting from the image calculates for each column the DSD. Then, the algorithm finds the columns whose DSD values are greater than a t_H threshold and promotes all these columns as belonging to the ROI. Next, for each of the columns belonging to the ROI, the algorithm finds the adjacent columns whose DSD values are greater than t_L and promotes also these columns as belonging to the ROI. If ROI of areas close to the edge of the tube must be excluded from the analysis, the algorithm removes from the ROIs the columns adjacent to the first and the last column.

The choice of the threshold values used in the algorithm determines algorithm performance. It can cause the exclusion of defects in the ROIs (causing false negative in detection), or it can generate too large ROI with no reduction of the overall processing time.

The choice of threshold t_H must guarantee that at least one column of a defect belongs to the ROI, i.e. the DSD for that column is higher than t_H. To ensure that all the defects are correctly included in the ROI, the threshold t_H must be chosen lower than the maximum values of the DSD of the columns of all the defects. As t_H threshold increases, the number of zones included in the ROI decreases. Too high values of t_H can exclude from the ROI areas that include defects. As t_H threshold decreases, the number of zones included in the ROI increases. Too low values of t_H, therefore, lead to extremely large ROI.
The choice of threshold t_L must guarantee that all the columns of a defect belong to the ROI, otherwise a portion of the defect are not detected, thus limiting the quality of detection. Too high value of t_L could exclude portions of the shape of the defect from the ROI. Too low values of t_L could cause again the ROI to include the entire internal of the tube. A possible solution is to set it to a value lower than the minimum value of the DSD of the columns of all the defects. This ensures that, if a defect is detected using threshold t_H, its entire shape is included in the ROI.

The thresholds t_L and t_H used by the algorithm are related to properties of defects that depends on production-related parameters (such as glass tube size, diameter, thickness, opacity etc). In an industrial application scenario, these parameters change with batches of production, so it is important to adapt the thresholds to the changes in production. We have developed a procedure that suggests upper bounds for the thresholds that must be adopted when the production parameters change.

The procedure consists of:

1) collecting several frames from the acquisition system during the production switches
2) applying any algorithm for the detection and classification of defects to each frame
3) for each classified defect, calculating the maximum value and minimum value of the DSD of the columns of the defect and adding them respectively to the sets maxDSD and minDSD
4) the suggested upper bounds are: $t_L < \min(\text{minDSD})$ and $t_H < \min(\text{maxDSD})$.

TABLE I
HOST COMPUTER

Hardware Configuration			
Processor	*Intel*® Core™ i7-*940* Processor (8MB Cache, 2.93 GHz)		
RAM	8 GB		
Defect detection system			
Algorithm name	Without DSDRR	DSDRR with edges	DSDRR no edges
ROI extraction	Internal part	Internal part + DSDRR including edges with t_L=0, t_H=2	Internal part + DSDRR excluding edges with t_L=0, t_H=2
Defect Detection Implementation	Canny (35,80) or MAGDDA (ws = 145, k=10.7)		
	OPENCV		

5. RESULTS

The inspection system has been implemented and it is working on production lines of a glass tube foundry [1]. The algorithm has been implemented in OpenCV [29], [30] and the image processing pipeline runs as a task activated by the frame grabber when a new frame is ready in main memory. Table I summarizes the main features of the Host Computer, the algorithms utilized for the various stages of defect detection and their configuration parameters. All the image processing algorithms have been implemented using the OpenCV library [29], [30] and compiled with the Visual Studio compiler.

System performance has been evaluated using a dataset of 30 frames acquired during the production phase. All frames are composed of 1000 lines acquired by the line scan camera sensor (2K pixels). These frames contain 6 air lines and 10 blobs; one of these frames contains 3 blobs and another one contains 2 air lines while 17 frames do not have any type of defects. The machine on which tests are executed has a configuration like the production one and is equipped with an Intel Core i7-940 CPU running at 2.93 GHz. As for processing time, we perform 1000 executions of the whole dataset of images [31], and we take the average execution time spent by each stage (ROI extraction/Defect detection/Defect Classification) and the maximum total processing time.

Our proposal is orthogonal to the specific defect detection algorithm. In our experiment, we utilized two algorithms that have been successfully applied in the inspection of pharmaceutical glass tube: the Canny algorithm [14] and the MAGDDA [32]. With Canny, the image is first smoothed with a Gaussian filter and then gradient magnitude is computed at each pixel; edges (marked pixels) are determined via non-maximum suppression, double threshold, and hysteresis. MAGDDA algorithm [32] works at row level and apply to the ROI a moving average filter of an assigned window. Then applies a fixed threshold (k), to mark the pixel.

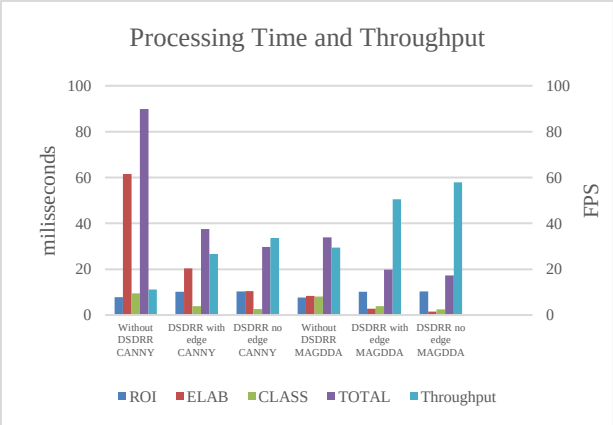

Fig.5 Processing Time and Throughput. ROI is the average processing time (a.p.t.) of the ROI extraction phase, ELAB is the a.p.t. of the defect detection algorithm, CLASS is the a.p.t. of the classification phase. TOTAL represents the worst-case overall processing time.

As for the Defect Classification stage, we adopt an algorithm that groups adjacent marked pixels using connected-components labeling and builds, for each group, the smallest rectangle that contains them. Measurements on the rectangle permits to individuate blobs and air lines.
In the tested image-set, the tuning procedure of Section 4 suggests for t_H a value less than 2,0362 and for t_L a value less than 0,0126. We set $t_H = 2$ and $t_L = 0$.

With this setting, in terms of defect detection (Tables II, where TP is the number of true positives, i.e. the number of defects that are properly classified by the algorithm; FP is the number of false positives, i.e. defects that are classified by the algorithm but that do not correspond to real defects in the tube; and FN is the number of false negatives, i.e. defects that are present in the tube but are not recognized by the algorithm; defective frames are the number of frames discarded with a similar classification), the accuracy of each defect detection algorithm is the same with or without the application of the DSDRR algorithm when including also the edges of the tube.

TABLE II
NUMBER OF RECOGNIZED DEFECTS/DEFECTIVE FRAMES AND THEIR CLASSIFICATION

	Expected value TP	Without DSDRR DSDRR with edge Canny TP/FP (FN)	DSDRR no edge Canny TP/FP (FN)	Without DSDRR DSDRR with edge - MAGDDA TP/FP (FN)	DSDRR no edge - MAGDDA TP/FP (FN)
Blobs	10	10/5 (0)	9/5 (1)	10/6 (0)	9/6 (1)
Air lines	6	6/0 (0)	6/0 (0)	6/0 (0)	6/0 (0)
Defective Frames	13	13/2 (0)	12/2 (1)	13/2 (0)	12/2 (1)

The DSDRR algorithm is effective in reducing the ROI that is processed by the Defect Detection and Classification algorithms. DSDRR calculates 70 ROIs. 53 of these are in the proximity of the edge of tube (and 1 of these contains a defect), 14 contain defects (3 defects are in the same columns/ROI). Compared to the area of the internal parts of the tube, the ROI is reduced on average by 88%, and at most by 96% and at least by 69%. Excluding the parts near the edges of the tube, the ROI is reduced on average by 98% and at most by 100% (in frames without defects) and at least by 82%. To further reduce the processing time, these results suggest excluding the investigation of the image edges. Indeed, the system is equipped with three cameras to guarantee a 360 degrees inspection of the tube, and defects near an image edge for a camera are located by one of the other cameras near the center of the image. So, the inspection quality is guaranteed.

The reduced area of the ROI has a direct impact on the processing time of the further stages of detection, and in the overall processing time (Fig. 5). The average execution time of Canny without DSDRR is about 61 ms while the execution time of Canny with DSDRR with edges is about 20 ms and 10 ms with DSDRR no edges, with a decrease of 67% and 83%. For MAGDDA, the execution time without DSDRR is 8.33 ms while with DSDRR with edges is about 3 ms and 2 ms with DSDRR no edges. Similar improvements can be observed for the processing time of the classification stage, as noisy pixels that do not belong to the DSDRR ROI are not considered in the Classification stage. The DSDRR algorithm increases the processing time for ROI extraction (from 8 to 10 ms). Despite this, the total maximum processing time for Canny moves from 90 to 37/30 ms (with a 3x increase in throughput) and for MAGDDA from 34 to 19/17 ms (with a 2x increase in throughput).

Since the processing period must be lower than the acquisition period, a reduction of the processing time allows the use of cameras with a higher sample rate or to increase the speed of production without loss of precision and accuracy in defects recognition.

6. CONCLUSION

A vision system can be exploited to inspect the quality of glass products during the production process. Improvements in such processes and the need to increase the accuracy of detection suggest the adoption of solutions that reduce the processing time of all the steps involved in defect detection and classification. A classical approach for dealing with inspection consists in extracting the whole internal part of the product (ROI) and pass it to defect detection and classification algorithm. In this paper, we proposed the idea of further reducing the ROI area by excluding columns that can be assumed to not include defects, with a consequent reduction in the processing time. As a proof of concept, we apply the idea to the inspection of pharmaceutical glass tubes. By considering the features of defects and properties that are relevant in such domain, we derive that Detrended Standard Deviation can be exploited to compensate the effects of not perfect alignment of camera and illuminator, and we utilize a double threshold with hysteresis algorithm to detect column belonging to the ROI that must be investigated. Experimental results indicate that our proposal does not change the quality of detection of the system and significantly improves processing time of both defect detection and classification stages. The overall throughput is improved up to 3 times.

The idea of reducing the ROI is general: as for future works, we plan to quantify its effectiveness in other application domains, and to investigate strategies to parallelize the algorithms by considering advanced CMPs and the GPU architectures and their memory hierarchy [33].

7. ACKNOWLEDGMENTS

This work has been partially supported by the Italian Ministry of Education and Research (MIUR) in the framework of the CrossLab project (Departments of Excellence – LAB Advanced Manufacturing and LAB Cloud Computing, Big data &

Cybersecurity)

8. REFERENCES

[1] P. Foglia, C.A. Prete, M. Zanda, An inspection system for pharmaceutical glass tubes, WSEAS Transactions on Systems, Vol. 14, Art. #12, PP. 123-136, 2015

[2] Kumar, Ajay. "Computer-vision-based fabric defect detection: A survey. "IEEE trans. on ind, electronics 55.1 (2008): 348-363.

[3] Peng, Xiangqian, et al. An online defects inspection method for float glass fabrication based on machine vision. The International Journal of Advanced Manufacturing Technology 39.11-12 (2008): 1180-1189.

[4] S. Campanelli, P. Foglia, C.A. Prete. An architecture to integrate IEC 61131-3 systems in an IEC 61499 distributed solution, Computers in Industry, Vol. 72, Sept. 2015, pp. 47-67.

[5] P. Foglia, et al. Towards relating physiological signals to usability metrics: A case study with a web avatar (2014) WSEAS Transactions on Computers, 13, pp. 624-634.

[6] Reynolds G, Peskiest D. Glass delamination and breakage, new answers for a growing problem; BioProcess International 9(11):52-57, 2011.

[7] Iacocca R.G., Toltl N., et al.. Factors Affecting the Chemical Durability of Glass Used in the Pharmaceutical Industry. AAPS PharmSciTech, v.11(3):1340-1349, 2010.

[8] Schaut, Robert A., and W. Porter Weeks. "Historical review of glasses used for parenteral packaging." PDA journal of pharmaceutical science and technology, 71.4 (2017): 279-296.

[9] Berry H. Pharmaceutical aspects of glass and rubber; J. of Pharmacy and Pharmacology, v.5(11):1008-1023; Wiley, 2011.

[10] Martínez, S. Satorres, et al. "An industrial vision system for surface quality inspection of transparent parts." The International Journal of Advanced Manufacturing Technology 68.5-8 (2013): 1123-1136

[11] Malamas, N., et al. "A survey on industrial vision systems, applications and tools." Image and vision computing 21.2 (2003): 171-188.

[12] Li, Di, Lie-Quan Liang, and Wu-Jie Zhang. "Defect inspection and extraction of the mobile phone cover glass based on the principal components analysis." The International Journal of Advanced Manufacturing Technology 73.9-12 (2014): 1605-1614.

[13] Kumar, Mukesh, Rohini Saxena. "Algorithm and technique on various edge detection: A survey." Signal & Image Processing 4.3 (2013): 65.

[14] J.F. Canny, A computational approach to edge detection, IEEE Trans. Pattern Analysis and Machine Intelligence, 8(6):679–698, 1986

[15] N.G. Shankar, Z.W. Zhong, Defect detection on semiconductor wafer surfaces, Microelectronic Engineering, 77 (3–4), 337-346, 2005

[16] Adamo, Francesco, et al. "A low-cost inspection system for online defects assessment in satin glass." Measurement 42.9 (2009): 1304-1311.

[17] Xinbo Huang, et al, An Online Technology for Measuring Icing Shape on Conductor Based on Vision and Force Sensors, IEEE Transactions on Instrumentation and Measurement, 66 (12) 3180-3189, 2017.

[18] M.M. de Beer, et al., Bubble formation in co-fed gas–liquid flows in a rotor-stator spinning disc reactor, International Journal of Multiphase Flow, Volume 83, 2016, pp 142-152.

[19] Saxena, Lalit Prakash. "Niblack's binarization method and its modifications to real-time applications: a review." Artificial Intelligence Review (2017): 1-33.

[20] Otsu N, A threshold selection using an iterative selection method. IEEE Trans Syst Man Cybern (1979) 9:62–66

[21] Zouhir Wakaf, Hamid A. Jalab, Defect detection based on extreme edge of defective region histogram, Journal of King Saud University - Computer and Information Sciences, Volume 30, Issue 1, 2018, Pages 33-40

[22] L. Huai-guang et al., A classification method of glass defect based on multiresolution and information fusion, The International Journal of Advanced Manufacturing Technology, Vol. 56 (9), pp. 1079-1090, 2011.

[23] Masoumeh Aminzadeh, Thomas Kurfess, Automatic thresholding for defect detection by background histogram mode extents, Journal of Manufacturing Systems, Vol. 37(1), pp. 83-92, 2015.

[24] H. Kong, et al., "Accurate and Efficient Inspection of Speckle and Scratch Defects on Surfaces of Planar Products," IEEE Trans. on Industrial Informatics, vol. 13(4), pp. 1855-1865, Aug. 2017.

[25] Farid, S., and F. Ahmed. "Application of Niblack's method on images." Inter. Conf. on Emerging Technologies. IEEE, 2009.

[26] Kim, Churl Min, Sung Ryul Kim, and Jung Hwan Ahn. "Development of Auto-Seeding System Using Image Processing Technology in the Sapphire Crystal Growth Process via the Kyropoulos Method." Applied Sciences 7.4 (2017): 371.

[27] J. Sauvola, M. Pietikäinen, Adaptive document image binarization, Pattern Recognition, Vol. 33(2), 2000, pp 225-236.

[28] Kulyukin V, Kutiyanawala A, Zaman T (2012) Eyes-free barcode detection on smartphones with Niblack's binarization and support vector machines. Proc Int Conf Image Process Comput Vis Pattern Recognit 1:284–290

[29] Bradski, Gary, and Adrian Kaehler. Learning OpenCV: Computer vision with the OpenCV library. O'Reilly Media, Inc., 2008.

[30] https://opencv.org/

[31] J. Abella, M. Padilla, et al., Measurement-Based Worst-Case Execution Time Estimation Using the Coefficient of Variation, ACM Trans. Des. Autom. Electron. Syst.22, 4, Article 72 (June 2017).

[32] G.A. De Vitis, P. Foglia, C.A. Prete, "A Special Purpose Algorithm to Inspect Glass Tubes in the Production Phase", TR-DII-2018-01, University of Pisa, 2018

[33] Bartolini, S., Foglia, P., & Prete, C. A. (2018). Exploring the relationship between architectures and management policies in the design of NUCA-based chip multicore systems. Future Generation Computer Systems, 78, 481–501.